A Stochastic Geometry approach to performance modeling of SWIPT vehicular networks

Gianluca Rizzo
HES-SO Valais, Switzerland &
University of Foggia, Italy
gianluca.rizzo@hevs.ch

Biagio Boi
Christian Esposito
University of Salerno, Italy
bboi@unisa.it
esposito@unisa.it

Marco Ajmone Marsan
Institute IMDEA Networks, Spain
marco.ajmone@polito.it

***Abstract*—With the increasing number of devices and the advent of 5G and 6G networks, ensuring reliable power and data connectivity remains a significant challenge, particularly in rural or remote areas. Simultaneous Wireless Information and Power Transfer (SWIPT) networks have emerged as a promising solution to power devices without batteries. However, their deployment in real-world scenarios is hindered by complex channel conditions and spatial dynamics. This research introduces a two-tier analytical model grounded in stochastic geometry, where base stations (BSs) are arranged along roads following a Poisson Line Cox Process (PLCP), while user equipment (UEs) is distributed using a Poisson Point Process (PPP). A comparative evaluation against planar PPP-based models demonstrates the performance advantages of this novel approach. Additionally, a Genetic Algorithm (GA) is applied to explore real-world scenario parameters, enhancing the model's adaptability and performance in practical applications.**

I. Introduction

The rapid evolution of wireless communication technologies has ushered in an era where connectivity is ubiquitous, driven by the increasing demand for higher data rates, low latency, and extended battery life. In such a context, IoT devices play a fundamental role in smart applications in urban and rural areas, where the latter have trouble guaranteeing reliable and stable power and data connectivity. For this reason and for efficiency reasons, such as power neutrality and reduced space available on board, interest in technologies that are able to power up devices without a battery is increasing. Among these solutions, Wireless Power Transfer (WPT) is one of the most popular ones.

WPT can be useful in a context where connectivity is offered by other media but in post-disaster or remote scenarios, Simultaneous Wireless Information and Power Transfer (SWIPT) networks are considered as one of the most interesting technologies over the last few years. The huge challenge is that SWIPT cannot be applied without a well-defined system using parameters that can easily be adapted in a real-world scenario. Characterization and performance evaluation of SWIPT networks is inherently complex due to the interplay of spatial dynamics, stochastic channel conditions, and energy harvesting capabilities. Traditional analytical methods often struggle to capture the nuanced behaviors of these networks under real-world conditions. Consequently, there is a growing interest in leveraging Stochastic Geometry (SG)—a powerful mathematical framework for modeling spatially distributed systems—to provide accurate performance assessments in SWIPT environments [1].

The advent of the automotive industry, 5G and future 6G drastically increased the number of devices [2] leading to new opportunities within the context of smart devices and network modelization. UAVs (Unmanned Aerial Vehicles) can be used to power up IoT devices in post-disaster scenarios [3], and a correct modelization of the network is necessary to correctly configure the parameters. It is possible to imagine a context where devices are not directly connected to the Internet but can leverage vehicle connections for sending information. If on one side, the Poisson Point Process (PPP) is a well-defined framework in network coverage and analysis [4], this cannot be automatically turned into a SWIPT system due to the power parameters involved. Moreover, by placing BSs on roads, rather than on the plan according to a PPP, some differences will be introduced on statistics and performance perceived by the users.

Driven by the evolution of SWIPT systems and the need to develop increasingly reliable analytical models, this research aims to evaluate vehicular SWIPT networks, focusing on key insights. The main contributions of this work can be summarized as follows:

- Development of a two-tier analytical model for SWIPT networks, where BSs are placed along lines following a Poisson Line Cox Process (PLCP), and User Equipments (UEs) are distributed according to a PPP;
- Formulation of an optimization problem targeting power consumption minimization by fine-tuning key architectural parameters of the network;
- Comparative evaluation of the proposed model against a planar PPP-based SWIPT network, to assess the impact of the new characterization and to highlight its advantages and limitations.

Moreover, the proposed architecture will be evaluated using a Genetic Algorithm (GA) designed to efficiently explore a set of real-world scenario parameters and constraints.

II. Related Works

SG is a mathematical framework, where a key subject is the representation of random point patterns in a space. The

current literature is rich in applications of such a theory for the study and analysis of wireless, cellular, and ad-hoc networks, such that the following surveys and tutorials have been published [5]–[10]. All these past experiences have in common that SG methods are used to model partial statistical property-based performance parameters (interference, throughput, etc.). Such models can be exploited to study and resolve different challenged related to wireless, cellular, and ad-hoc networks, such as node or user position, user association, state control, power measurements, etc.

Among the first works within the application of PPP to the wireless networks we found [11], where a cellular network model is composed of base stations (BSs) arranged according to some homogeneous PPP in the Euclidean plane; assuming that mobile user is associated with the closest base station. Baccelli concludes the work in [11] with multiple considerations on the Fading, highlighting a general fading with noise using $\alpha = 4$, and general fading without noise with $\alpha > 2$. The work is a milestone for the downlink cellular network analysis, with possible applications in the C-RANs network composed of micro/pico and femtocells, where user distance and cell size are the most relevant parameters. In [12], considerations on macro cell demonstrate the PPP is not usable in the context where BSs are deployed close to each other and possible usage of the Determinantal Point Process (DPP) can extend the theory proposed in the previous work. New generation C-RAN leverage on micro, pico, and femtocells; where macro cells are not employed and it is possible to use PPP.

The usage of SG to model SWIPT networks has already been evaluated for Non-orthogonal multiple access (NOMA) technique in [13] while a first evaluation in IoT context has been proposed in [14], where devices harvest energy from the surrounding environment, from both BSs and User Equipments (UEs). Anyway, new generations of C-RANs are deployed considering the case of vehicles and the greatest part of the discussed research in the context of SWIPT does not take into consideration the mobility of nodes, meaning that both the devices and BSs are assumed to be stationary and do not move in space. [15] considers the case of a dense IoT environment that leverages vehicles to exchange data and deliver wireless connectivity. In [16], the vehicles are considered activators of IoT devices and can be used for transmitting data. Each vehicle has a coverage risk of radius centered at the vehicle, while IoT devices are distributed according to a related PPP. In [17] the authors modeled the source of power or more generally the BSs using PPP, while a Manatthan Poisson Line Process (PLP) is used for modeling the walls, and so the fading. Considering the case of dense context, the results show an important impact of walls while there is no effect on the maximum achievable information rate by tuning the power splitting ratio.

Analysis of the literature underscores the widespread adoption of SG as a powerful tool for modeling and analyzing SWIPT networks, particularly in wireless communication scenarios. However, there remains a significant gap in research when applying SG to vehicular environments, where BSs are placed along roadways to support mobile users in dynamic traffic conditions. Existing studies largely focus on traditional fixed-network architectures, leaving the intricacies of vehicular networks — such as variable network topology, high mobility, and environmental factors — underexplored. This manuscript aims to bridge this gap by presenting a comprehensive SG-based approach tailored for SWIPT-enabled vehicular networks, offering insights into performance metrics specific to these scenarios.

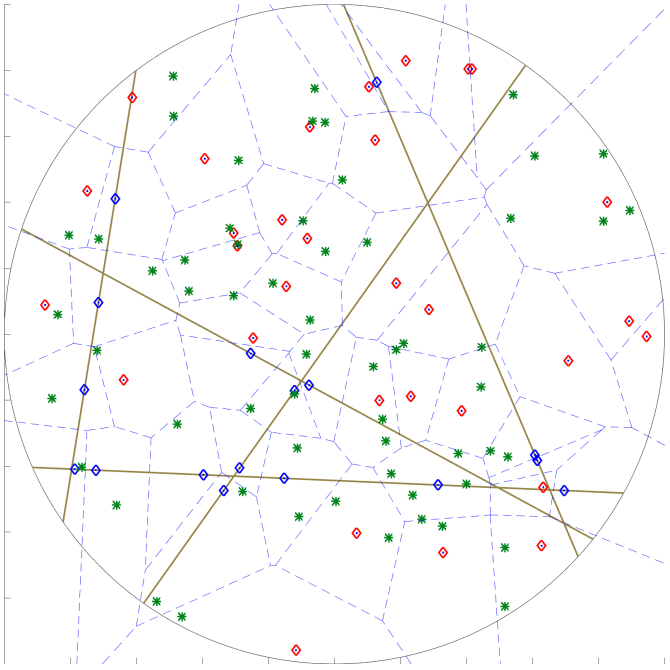

Fig. 1: Two tiers proposed architecture composed by UE (green), vehicular BS (blue) placed on roads (yellow), and planar BS (red).

III. System Model

For the purpose of our study, we consider a two-tier network containing two different distributions of Base Stations (BSs), while UEs are distributed in space according to Poisson Point Process (PPP) with a density λ_u. UEs are either broadband (BB) terminals, or IoT (Internet of Things) devices. We assume the latter are a fraction γ of the total number of UEs. Regarding the Base Station (BS), these are distributed into two tiers, and can be of two types: planar or vehicular, and are independently distributed into the space, according to two different processes.

Name	Description
Φ_b, Φ_u	Planar BSs and Planar UEs distribution
λ_b, λ_u	Planar BSs and Planar UEs density
Ψ_b	Vehicular BSs distribution
$\lambda_l \mu_b$	Vehicular BSs density
η	Splitting Factor

TABLE 1: Main notation used in the paper

Planar BS (PBS). In the first tier, the BSs are distributed according to a 2D homogeneous PPP Φ_b with a density λ_b.

Vehicular BS (VBS). In the second tier, a road system is modeled by an independent Poisson Line Process (PLP) $\Phi_l \in R^2$ produced by a homogeneous PPP Ξ on the cylinder $C := R[0, \pi)$ with an intensity λ_l. More precisely, a point of Ξ, denoted by (r_i, θ_i), describes the line $l_i \in R^2$ of equation

$$l(r_i, \theta_i) = \{(x, y) \in R^2 | xcos(\theta_i) + ysin(\theta_i) = r_i\} \quad (1)$$

where the parameters r and θ correspond to the shortest distance from the origin to the line and the angle between the positive x-axis and the line l, respectively. Conditionally on the lines, BSs are modeled by independent 1-D homogenous PPP with intensity μ_b, so the distance between two consecutive points on the same line hence follows the exponential distribution with parameter μ_b. The result is a *Poisson Line Cox Point Process* Ψ_b with spatial intensity which can be expressed as

$$\Lambda(A) = \mathbb{E}[N_p(A)|\Psi_b] = \mu_b \sum_{l_i \in \Psi_b} v_1(l_i \cap A) = \mu_b \pi \lambda_l \quad (2)$$

A. Coverage Analysis

We can evaluate the coverage probability of the proposed network, by using a three steps approach. This coverage probability is the fundamental measure, needed to evaluate all the performance measures, that will be discussed in the following subsections.

Step 1: Relevant distance distributions. The key distributions that are of interest for our analysis are the CDF and PDF of the distances between UE and the candidate serving BS from Tier 1 or Tier 2. Let us denote these distances with typical BS on Tier 1 with x_1 and with the typical BS on Tier 2 with x_2, which are driven by the random variable R_1 and R_2, respectively. As ϕ_b is an 2D homogeneous PPP, the CDF and PDF of R_1 are given by:

$$F_{R_1}(r_i) = 1 - \exp(-\lambda_b \pi r_i^2)$$
$$f_{R_1}(r_i) = 2\pi\lambda_b r_i \exp(-\lambda_b \pi r_i^2)$$

While in the Tier 2, since BS are distributed according to a PLCP Ψ_b, the CDF and PDF are given by:

$$F_{R_2}(r_i) = 1 - \exp\left[-2\pi\lambda_l \int_0^{r_i} \left(1 - \exp(-2\mu_b\sqrt{r_i^2 - \rho^2})\right) \mathrm{d}\rho\right]$$

$$f_{R_2}(r_i) = \left[2\pi\lambda_l \int_0^{r_i} \frac{2\mu_b r_i}{\sqrt{r_i^2 - u^2}} \exp(-2\mu_b\sqrt{r_i^2 - u^2})\, \mathrm{d}u\right] \times$$
$$\times \exp\left[-2\pi\lambda_l \int_0^{r_i} \left(1 - \exp(-2\mu_b\sqrt{r_i^2 - \rho^2})\right) \mathrm{d}\rho\right]$$

Step 2: Association probabilities. To derive the coverage probability we have to define the association probabilities to both the BSs belonging to the two tiers. Let us define E_1 the event in which the user is associated with a BS on the Tier 1, and with E_2 the event in which the user is associated with a BS on the Tier 2. The event E_1 occur when the distance from the nearest BS on the Tier 2 is greater than the distance of the BS on the Tier 1, so the probability of occurrence of the event E_1 can be computed as:

$$\begin{aligned}\mathbb{P}(E_1) &= \mathbb{P}(R_1 < R_2) \\ &= \mathbb{E}_{R_1}\Big[\mathbb{P}(R_2 > r_1 | R_1)\Big] \\ &= \int_0^\infty \Big(1 - F_{R_2}(r_1)\Big) f_{R_1}(r_1)\, \mathrm{d}r_1 \\ &= \int_0^\infty 2\pi\lambda_b r_1 e^{-\lambda_b \pi r_1^2 - 2\pi\lambda_l \int_0^{r_1} 1 - e^{-2\mu_b\sqrt{r_1^2 - \rho^2}}\, \mathrm{d}\rho}\, \mathrm{d}r_1\end{aligned} \quad (3)$$

While, the probability of being associated with a BS on the Tier 2 will be $\mathbb{P}(E_2) = 1 - \mathbb{P}(E_1)$. It is possible to notice that these probability also correspond to the probability to be associated to one of the two distribution, so we have that $\mathbb{P}(X \in \phi_b) = \mathbb{P}(E_1)$.

Step 3: Serving BS distance distribution. After computing the association probability to one among vehicular or planar BS, we can now proceed to the computation of the serving distance R and to the minimum of them in order to understand which is the final serving distance distribution among two different type of BS. R_1 and R_2 are two independent random variable, so the resulting minimum is a new random variable $U = min\{R_1, R_2\}$ whose CDF can be computed as follows.

$$\begin{aligned}F_U(r_i) &= 1 - (1 - F_{R_1}(r_i))(1 - F_{R_2}(r_i)) \\ F_U(r_i) &= 1 - (e^{-\lambda_b \pi r_i^2})(e^{-2\pi\lambda_l \int_0^{r_i} (1 - \exp(-2\mu_b\sqrt{r_i^2 - \rho^2}))\, \mathrm{d}\rho}) \\ F_U(r_i) &= 1 - e^{-\lambda_b \pi r_i^2 - 2\pi\lambda_l \int_0^{r_i} (1 - \exp(-2\mu_b\sqrt{r_i^2 - \rho^2}))\, \mathrm{d}\rho}\end{aligned} \quad (4)$$

While the PDF can be computed as the derivate in r_i of F_U

$$\begin{aligned}f_U(r_i) = 2\pi\lambda_b r_i e^{-\pi\lambda_b r_i^2 - 2\pi\lambda_l \int_0^{r_i} \left(1 - e^{-2\mu_b\sqrt{r_i^2 - t^2}}\right) \mathrm{d}t} \\ + e^{-\lambda_b \pi r_i^2 - 2\pi\lambda_l \int_0^{r_i} (1 - e^{-2\mu_b\sqrt{r_i^2 - \rho^2}})\, \mathrm{d}\rho} \\ \times \int_0^{r_i} \frac{4\lambda_l \pi \mu_b r_i e^{-2\mu_b\sqrt{r_i^2 - u^2}}}{\sqrt{r_i^2 - u^2}} du.\end{aligned} \quad (5)$$

B. Base station energy consumption and service model

According to our previous research in this context [18], a BS energy model, by which the power consumed by a BS, denoted as P_{BS}, is given by the following expression:

$$P_{BS} = q_1 + U_d[q_2 + q_3(P - P_{min})] \quad (6)$$

The expression is composed of a fixed part, which depends on the cost for the deployment of the BS itself, indicated as q_1 and by two components q_2 and q_3 depending on the utilization and the transmitting power used. For sake of completeness, we considered tha same costs for both planar and vehicular BSs, aiming at demonstrating the impact of the deployment of one of the two, independently from the costs that each of them leverage on. We can now define the capacity of the channel as follow:

$$C(r, P, G, I) = \frac{B}{k} \log_2\left(1 + \frac{PGr^{-\alpha}}{N_0 + I(r, k)}\right) \quad (7)$$

C. User Performance

In this section, we characterize the main performance parameters as a function of the main system parameters and the expression derived in the coverage analysis section.

Theorem 1. The mean ideal per-bit delays in downlink and uplink, and the mean ideal per-Joule delay perceived by a typical best-effort user joining the system are given by:

$$\bar{\tau}_d = H(w_d, w_d, C(r, P, G, \bar{I})) \tag{8}$$

$$\bar{\tau}_{d,I,TS} = \bar{\tau}_d \frac{w_d}{(1-\eta)} \tag{9}$$

$$\bar{\tau}_{d,I,PS} = H(w_d, 1, C(r, (1-\nu)P, G, (1-\nu)\bar{I})) \tag{10}$$

$$\bar{\tau}_u = H\left(\delta_u, \delta_u, C(r, P_I, 1, 0)\right) \tag{11}$$

$$\bar{\tau}_{u,I} = \delta_u \bar{\tau}_u \tag{12}$$

Where:

$$H(y, z, g(r)) = \int_0^\infty \frac{f(r, y) k(r)}{z g(r)} \, \mathrm{d}r. \tag{13}$$

with

$$f(r, y) = \lambda_u \left[y + \gamma\left(\phi - y\right)\right] \times$$

$$\times \int_0^\infty \int_0^{2\pi} e^{-\lambda_b A(r,x,\theta) - 2\pi\lambda_l \int_0^\rho 1 - e^{-2\mu_b \sqrt{\rho^2 - t^2}\, \mathrm{d}t}} x \, \mathrm{d}\theta \, \mathrm{d}x$$

$A(r, x, \theta)$ is the area of the circle centered at (x, θ) with radius x that is not overlapped by the circle centered at $(0, -r)$ with radius r. ρ is the radius of a circle with the same area $A(r, x, \theta)$. $C(r, P, G, \bar{I})$ is given by (7), with the interference term $\bar{I}$ given by

$$\bar{I}(r, k) = \frac{P L_g (\lambda_b + \lambda_l \mu_b) 2\pi r^{2-\alpha}}{k(\alpha - 2)} \frac{\bar{\tau}_d}{\tau_d^0} \tag{14}$$

Anyway, since we are considering a SWIPT network, it is important to model the energy received from a typical IoT device, can be harvested both from other UEs, and from other BSs, as well as from the connected BS.

Theorem 2. In the dense IoT regime, the cumulative distribution function CDF_h of the power harvested by an IoT user who is just beginning service is

$$CDF_h(h_0) = CDF_r(g^{-1}(h_0))$$

for all $h_0 \geq 0$, where CDF_r is the cumulative distribution function of the distance of the user to its serving BS:

$$CDF_r(r) = \int_0^r 2\pi\lambda_b r e^{-\lambda_b \pi r^2 - 2\pi\lambda_l \int_0^r (1 - a(r,u))\, \mathrm{d}u}$$

$$+ e^{-\lambda_b \pi r^2 - 2\pi\lambda_l \int_0^r (1 - a(r,u))\, \mathrm{d}u}$$

$$\times \int_0^r \frac{4\lambda_l \pi \mu_b r a(r, u)}{\sqrt{r^2 - u^2}} \, \mathrm{d}u \, \mathrm{d}r,$$

where

$$a(r, u) = e^{-2\mu_b \sqrt{r^2 - u^2}}$$

$$g(r) = \Theta\left(F_{TS}(r) + \frac{Z_{TS}(r)}{f(r, w_d)}\right)$$

with F_{TS} representing the energy harvested from the connected BS, and Z_{TS} representing the energy harvested from all the other BSs, as well as from the other UEs near the UE. These can be computed as follows, while $f(r, w_d)$ is given by Theorem 1.

$$F_{TS}(r) = P r^{-\alpha} L_g \frac{\bar{\tau}_d}{\tau_d^0} + k\bar{I}(r, k) + \bar{O}$$

$$Z_{TS}(r) = \frac{\bar{\tau}_d}{\tau_d^0}\left[P r^{-\alpha}(G\eta - L_g) - (1-\eta)(k\bar{I}(r, k) + \bar{O})\right]$$

$$\bar{O} = \frac{(1-\gamma)\delta_u P_{bb} + \phi\gamma P_I}{(1-\gamma)\delta_u + \phi\gamma} \frac{(\lambda_b + \lambda_l \mu_b)\pi\alpha}{\alpha - 2} \frac{\bar{\tau}_u}{\tau_u^0}$$

IV. Optimization Problem

Typically, in SWIPT networks it is hard to establish a unique setting for the main system parameters. This is because multiple configurations can achieve the same result. To determine the best configuration, we introduce here an optimization problem, which aims at reducing the total network power consumption in terms of transmitting power P, PBS density λ_b, VBS density μ_b and splitting factor for a given user density λ_u.

Problem 1.

$$min_{P, \lambda_b, \mu_b, \eta} \;\; \lambda_b + \pi\lambda_l\mu_b \Bigg[q_1 + \frac{\bar{\tau}_d(\eta, P, \lambda_b, \mu_b)}{\tau_d^0} \times$$

$$\times \left(q_2 + q_3(P - P_{min})\right)\Bigg]$$

$$\text{Subject to: } \frac{\bar{\tau}_d(\eta, P, \lambda_b)}{\tau_d^0} \leq 1, \quad \frac{\bar{\tau}_u(\eta, P, \lambda_b)}{\tau_u^0} \leq 1 \tag{15}$$

$$P_{min} \leq P \leq P_{max} \tag{16}$$

$$0 \leq \eta \leq 1 \tag{17}$$

$$CDF_h(h_0, \eta, P) \leq \mu \tag{18}$$

$$0 \leq \lambda_b \leq \lambda_{b,max} \tag{19}$$

$$\pi\lambda_l\mu_b > \varpi\lambda_b \tag{20}$$

where h_0 in constraint (18) is the minimum harvested power required by each IoT device to operate, computed based on the amount of energy required by the device during a whole on-off cycle. μ is the maximum acceptable ratio of IoT users which harvest less than h_0 Joules per second. $\bar{\tau}_d$, $\bar{\tau}_u$ are given by Theorem 1. $\lambda_{b,max}$ derives from practical constraints to BS deployments in urban settings. Finally, we considered a constraint on vehicular BSs in (20), which forces the optimization problem to consider a minimum amount of vehicular BSs. This constraint has been considered due to the generally better performance of PPP, with respect to PLCP.

In addressing the proposed problem, we employed a Genetic Algorithm (GA)-based approach, described in Algorithm 1 due to its strength in avoiding local minima by working with a population of potential solutions. In particular, we executed the GA by selecting the dominant chromosome (i.e., the one with the highest fitness value on the problem). The algorithm then generates a new population through appropriate genetic operators, namely mutation and crossover. The mutation used in the proposed algorithm is the default one, namely the Gaussian

mutation, while the crossover employed by the proposed algorithm returns a child that lies on the line containing the two parents, a small distance away from the parent with the better fitness value in the direction away from the parent with the worse fitness value. Through MATLAB it is possible to set the distance for which goes, which in our case has been set to 1.9. The application of two operations generates a new population which is evaluated against a fitness function according to the objective function of Problem 1. This process is repeated over 150 generations or until the termination condition is met, which is defined as no improvement over 10 consecutive generations. Through this approach, guided by the fitness function, the GA performs a random exploration of the solution space, driven by the outcomes of the evolutionary operators.

Algorithm 1 Genetic Algorithm used for the resolution of Problem 1

1: Initialize population W with n random chromosomes $C_i = (P, \lambda_b, \mu_b, \eta)$
2: **repeat**
3: Evaluate fitness of each chromosome in W
4: Archive best solutions from W in an archive
5: Evaluate solutions in the archive and remove low-quality ones
6: Select parents from W based on fitness (e.g., roulette wheel selection)
7: Apply genetic operators (e.g., crossover and mutation) to produce offspring
8: Replace least fit individuals in W with offspring to have a new generation
9: **until** Any improvement in 10 generations

To enhance the convergence of GA, the fitness function is constructed using the penalty method. In this method, a penalty term proportional to the degree of violation of constraints (15) (downlink and uplink) and (18) is added to the objective function of 1. Constraints (16), (17), (19) and (20) are considered in the nature of chromosome. This ensures that the algorithm can explore values near the boundary of the feasible region of Problem 1.

V. Numerical Results

In this section, we evaluate the impact of the integration of PLCP in a SWIPT system. We limit our discussion to just one configuration of SWIPT.

A. Setup

Base stations work at a frequency of 1 GHz, and use a bandwidth of 50 MHz. We assume a percentage of IoT devices equal to 20% of the total number of UEs, a transmit power equal to 0.2 W for both IoT and BB UEs, a frequency reuse factor of 3, a beamforming gain equal to 10, which is assumed constant over the whole main lobe aperture of 45 degrees, and a path loss exponent α = 3, typical of urban areas. Regarding the harvesting model, we considered an EH model with a conversion efficiency of 0.9 with no lower/upper threshold. We assume the BS transmit power to vary between 1 and 11 W, and we set a target mean per-bit delay in downlink for BB (resp. IoT) UEs equal to 10^{-5}s (resp. 10^{-3} s), and in uplink equal to 10^{-4}s for all UEs, (e.g. typical of IoT systems for environmental monitoring [19]). We consider the user density to vary from 10^{-4} users per m^2 (typical of settings with a high share of BB users, at night) to 10^{-1} users per m^2 (modeling scenarios with crowds of BB UEs and with high density of IoT deployments). We assume IoT UEs to be active for all the time time ($\phi = 1$), while the minimum harvested power is 6mW. We set to 5% the maximum acceptable share of IoT users which are not able to harvest the target minimum energy. The parameters of the BS energy model are chosen to fit two different types of BSs. These BS reflects the behavior of the majority of current stand-alone BSs, and it is characterized by a 27% load proportionality (with q_1 = 1100, q_2 = 100, and q_3 = 30). For the evaluation we considered a single PPP distribution, and three PLCP distributions. The PLCP distribution are charactherized by different minimum amount of BS (0, 20, 40 %) over the total number of BS, as specified in the constraint (20) of Problem 1.

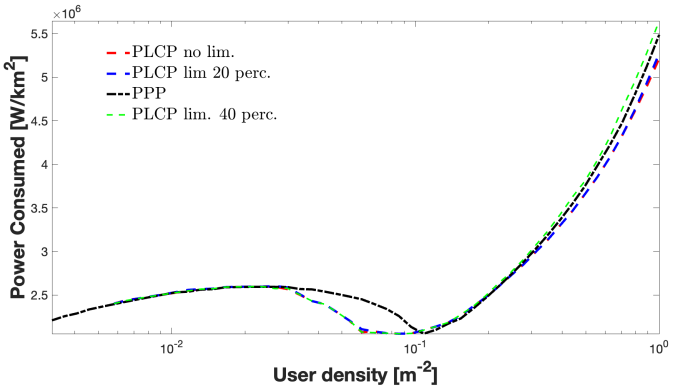

Fig. 2: Power per km^2 consumed by the network at the optimum vs user density, for different BS distributions.

B. Energy optimal configuration

In order to investigate the properties of the solutions of Problem 1, in Fig. 2 we plot the power per km^2 consumed by the network at the optimum, as a function of user density, while in Fig. 3 to 6 we plot the corresponding optimal values of vehicular and planar base station density, of transmit power, and of time split ratio.

A general consideration independently from the different kinds of BSs distribution is the exponential increase in power consumption for highly dense user density, due to the low load of these BS, while at low user densities, an energy-optimal tuning of the system brings to an almost linear proportionality between user density and consumed power. This is in part caused by the presence of a high number of BSs corresponding to high interference, which plays a crucial role in this evaluation. By carefully looking at the high user density, PLCP is able to marginally reduce the power consumed by the network, with respect to PPP for all the minimum amount except for

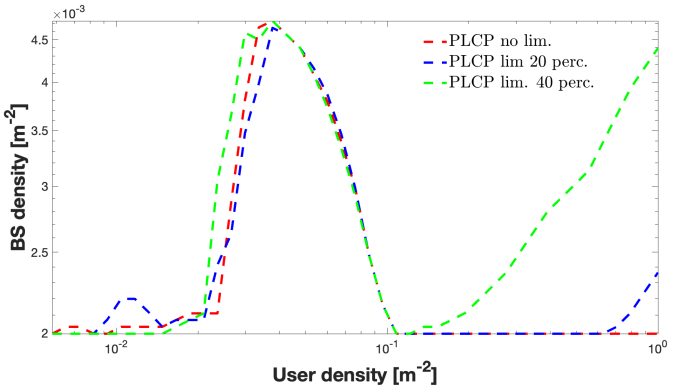

Fig. 3: Optimal vehicular base station density per km^2 for different BS distributions.

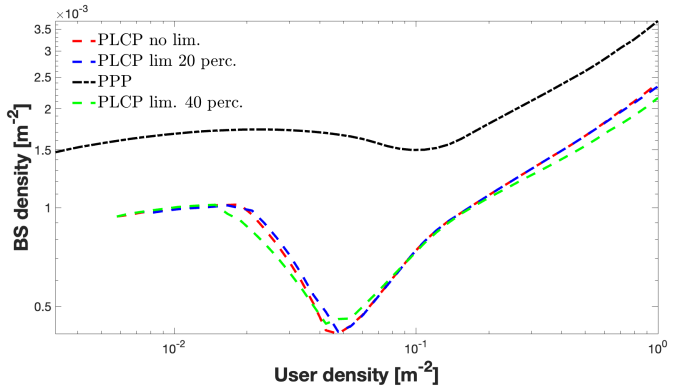

Fig. 4: Optimal planar base station density per km^2 for different BS distributions.

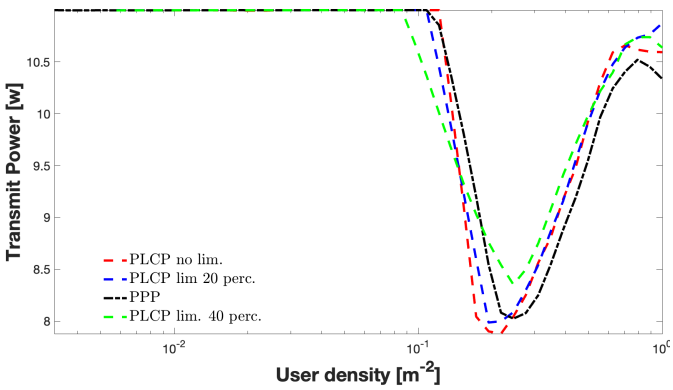

Fig. 5: Optimal BS transmit power for different BS distributions.

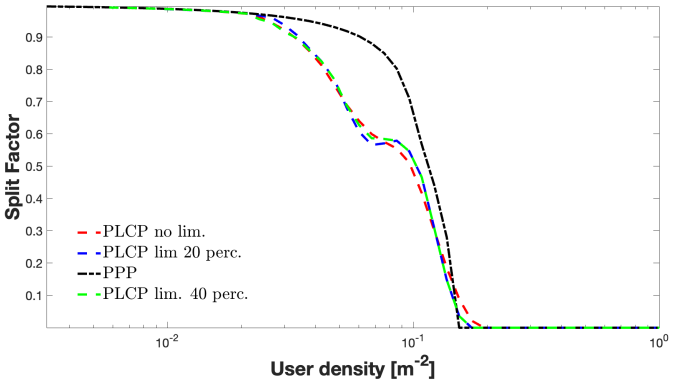

Fig. 6: Optimal splitting factor for different BS distributions.

40% configuration. This demonstrates the beneficial effect of PLCP, which by distributing BSs over lines instead of randomly in the space, such as PPP, is able to reduce the interference, and hence, increase the efficiency of the network. However, in sharp contrast to RANs delivering only connectivity, at high user densities the service capacity of a SWIPT network is complemented by the signals transmitted by users, which thus contribute to the delivery of power to IoT users. Despite at both lower and higher user density, there is no relevant difference between PPP and PLCP, by looking in the middle, in the area between 10^{-1} and 50^{-1}, an evident difference exists. The beneficial effect is particularly relevant for some densities as shown in Fig. 7, where PLCP is much more effective in leveraging the energy produced by the other users, rather than PPP. This is directly caused by the reduced amount of PBS deployed, as shown in Fig. 4. Fig. 5 and 6 offer some key insight on how tuning transmit power and power split ratio contributes to achieving energy optimal operation. The behaviour between PLCP and PPP is almost the same, with the only difference in the splitting factor, caused by the interference, as previously discussed.

VI. Conclusions

In this research, we demonstrated the effectiveness of the Poisson Line Cox Process (PLCP) distribution for the characterization of a SWIPT network composed of both broadband and IoT UEs. This representation enables the evaluation of a more realistic network, populated by vehicular devices such as UAVs. Results demonstrate some advantages in introducing vehicular BSs to avoid overlapping and hence increasing interference in the network. In the future, we want to assess the mean waiting time for transmission, referred to as the Age of Information (AoI), as an important metric to understand the quality of the harvesting process.

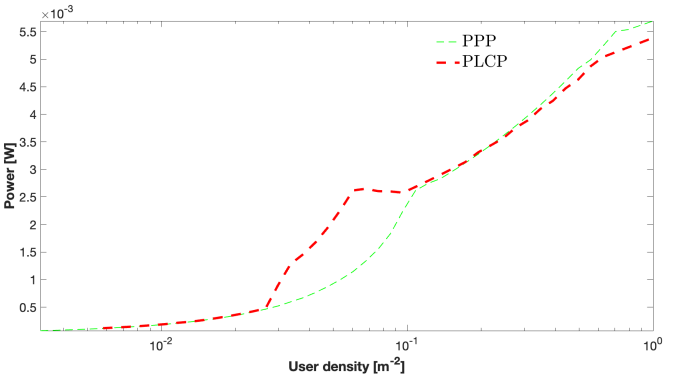

Fig. 7: Energy Harvested from other UEs vs. user density for different BS distributions.

ACKNOWLEDGMENT

This work was supported by the Korea Institute of Energy Technology Evaluation and Planning (KETEP) grant funded by the Korea government (MOTIE) (RS-2023-00303559, Study on developing cyber-physical attack response system and security management system to maximize real-time distributed resource availability)

REFERENCES

[1] R. Ma, J. Tang, X. Y. Zhang, W. Feng, D. K. C. So, C.-B. Chae, K.-K. Wong, and J. A. Chambers, "Simultaneous wireless information and power transfer in iot-based scenarios: Architectures, challenges, and prototype validation," *IEEE Wireless Communications*, pp. 1–7, 2024.

[2] S. Das and E. Mao, "The global energy footprint of information and communication technology electronics in connected internet-of-things devices," *Sustainable Energy, Grids and Networks*, vol. 24, p. 100408, 2020.

[3] C. Esposito and G. Rizzo, "Help from above: Uav-empowered network resiliency in post-disaster scenarios," in *2022 IEEE 19th Annual Consumer Communications & Networking Conference (CCNC)*, 2022, pp. 477–480.

[4] J. G. Andrews, A. K. Gupta, and H. S. Dhillon, "A primer on cellular network analysis using stochastic geometry," *CoRR*, vol. abs/1604.03183, 2016.

[5] N. Sharma and K. Kumar, "Resource allocation trends for ultra dense networks in 5g and beyond networks: A classification and comprehensive survey," *Physical Communication*, vol. 48, p. 101415, 2021.

[6] O. A. Amodu, M. Othman, N. K. Noordin, and I. Ahmad, "Relay-assisted d2d underlay cellular network analysis using stochastic geometry: Overview and future directions," *IEEE Access*, vol. 7, pp. 115 023–115 051, 2019.

[7] H. ElSawy, A. Sultan-Salem, M.-S. Alouini, and M. Z. Win, "Modeling and analysis of cellular networks using stochastic geometry: A tutorial," *IEEE Communications Surveys & Tutorials*, vol. 19, no. 1, pp. 167–203, 2016.

[8] S. D. Okegbile, B. T. Maharaj, and A. S. Alfa, "Stochastic geometry approach towards interference management and control in cognitive radio network: A survey," *Computer Communications*, vol. 166, pp. 174–195, 2021.

[9] X. Lu, M. Salehi, M. Haenggi, E. Hossain, and H. Jiang, "Stochastic geometry analysis of spatial-temporal performance in wireless networks: A tutorial," *IEEE Communications Surveys & Tutorials*, 2021.

[10] Y. Hmamouche, M. Benjillali, S. Saoudi, H. Yanikomeroglu, and M. Di Renzo, "New trends in stochastic geometry for wireless networks: A tutorial and survey," *Proceedings of the IEEE*, 2021.

[11] J. G. Andrews, F. Baccelli, and R. K. Ganti, "A tractable approach to coverage and rate in cellular networks," *IEEE Transactions on Communications*, vol. 59, no. 11, pp. 3122–3134, 2011.

[12] Y. Li, F. Baccelli, H. S. Dhillon, and J. G. Andrews, "Statistical modeling and probabilistic analysis of cellular networks with determinantal point processes," *IEEE Transactions on Communications*, vol. 63, no. 9, pp. 3405–3422, 2015.

[13] A. S. Parihar, P. Swami, and V. Bhatia, "On performance of swipt enabled ppp distributed cooperative noma networks using stochastic geometry," *IEEE Transactions on Vehicular Technology*, vol. 71, no. 5, pp. 5639–5644, 2022.

[14] G. Rizzo, M. A. Marsan, and C. Esposito, "Energy-optimal ran configurations for swipt iot," in *2022 20th International Symposium on Modeling and Optimization in Mobile, Ad hoc, and Wireless Networks (WiOpt)*, 2022, pp. 169–176.

[15] C.-S. Choi, F. Baccelli, and G. de Veciana, "Densification leveraging mobility: An iot architecture based on mesh networking and vehicles," in *Proceedings of the Eighteenth ACM International Symposium on Mobile Ad Hoc Networking and Computing*, ser. Mobihoc '18. New York, NY, USA: Association for Computing Machinery, 2018, p. 71–80.

[16] C.-S. Choi and F. Baccelli, "Modeling and optimization of direct communications from iot devices to vehicles," *2018 IEEE Globecom Workshops (GC Wkshps)*, pp. 1–7, 2018.

[17] A. I. Akin, I. Stupia, and L. Vandendorpe, "On the effect of blockage objects in dense mimo swipt networks," *IEEE Transactions on Communications*, vol. 67, no. 2, pp. 1059–1069, 2019.

[18] G. Rizzo, M. A. Marsan, C. Esposito, and B. Boi, "Green operations of swipt networks: The role of end-user devices," *arXiv preprint arXiv:2312.08232*, 2023.

[19] W. Lu, X. Xu, G. Huang, B. Li, Y. Wu, N. Zhao, and F. R. Yu, "Energy Efficiency Optimization in SWIPT Enabled WSNs for Smart Agriculture," *IEEE Trans. Ind. Inf.*, vol. 17, no. 6, pp. 4335–4344, Jun. 2021.

[20] B. Rengarajan, G. Rizzo, and M. A. Marsan, "Energy-optimal base station density in cellular access networks with sleep modes," *Computer Networks*, vol. 78, pp. 152–163, 2015.

[21] G. A. Rizzo and M. A. Marsan, "The energy saving potential of static and adaptive resource provisioning in dense cellular networks," in *IEEE COMSNETS*, 2018, pp. 297–304.

[22] D. Stoyan, W. S. Kendall, and J. Mecke, *Stochastic geometry and its applications*. Wiley, 1987.

APPENDIX

A. Proof of Theorem 1

Here we sketch the main steps of the proof. The derivation of the expression of the per-bit delay goes along the same lines as the proof of Theorem 3.1 in [20]. The main variants are the use of the palm expectation of $I(r,k)$, $\bar{I}(r,k,\bar{\tau})$, instead of $I(r,k)$, in order to make the derivation analytically tractable.

We consider the user at zero, but we drop this indication in what follows for ease of notation (i.e. $S(0)$ becomes S, and $D(0)$ becomes D). We start by computing the Palm expectation of the expression in representing the load of a single BS:

$$\bar{\tau}_d = E^0\left[\frac{N_{iot}(S)+w_d N_{bb}(S)}{w_d C(D,I)}\right]$$

$$= \int_0^\infty E^0[\tfrac{N_{iot}(S)+w_d N_{bb}(S)}{w_d C(D,I)} | r \le D \le r+dr] P(r \le D \le r+dr)$$

Let $k(r) = P(r \le D \le r+dr)$. Under the Palm distribution of Φ_u, the distribution of r, i.e. of the distance from the origin to the nearest base station, is given by the minimum of the two independent random variable representing the BSs distribution. Referring to expression in (5), it is possible to write:

$$k(r) = 2\pi\lambda_b r e^{-\pi\lambda_b r^2 - 2\pi\lambda_l \int_0^r \left(1-e^{-2\mu_b\sqrt{r^2-t^2}}\right) \mathrm{d}t}$$

$$+e^{-\lambda_b \pi r_i^2 - 2\pi\lambda_l \int_0^{r_i}(1-e^{-2\mu_b\sqrt{r_i^2-\rho^2}})\,\mathrm{d}\rho}$$

$$\times \int_0^{r_i} \frac{4\lambda_l \pi \mu_b r e^{-2\mu_b\sqrt{r^2-u^2}}}{\sqrt{r^2-u^2}} du.$$

The resulting formula is:
$\approx \int_0^\infty \frac{E^0[N_{bb}(S)+w_d N_{iot}(S) | r \le D \le r+dr]}{w_d C(r,\bar{I}(r,k))} k(r) dr$

where $\bar{I}(r,k)$ is the average interfering power for the typical user at r, recalling what is described in [21], it is possible to extend the approach to the multiple BSs distributions (planar and vehicular). It will be given by $\bar{I}(r,k) = \frac{PL(\lambda_b+\lambda_l\mu_b)2\pi r^{2-\alpha}}{k(\alpha-2)} \frac{\bar{\tau}_d}{\tau_d^0}$. Thus
$\bar{\tau}_d \approx \int_0^\infty \frac{E^0[N_{bb}(S)+w_d N_{iot}(S) | r \le D \le r+dr]}{w_d C(r,\bar{I}(r,k))} k(r) dr$

Let $N_{tot}(S) = N_{bb}(S) + N_{iot}(S)$. The palm expectation at the numerator becomes

$$Q E^0[N_{tot}(D) | r \le D \le r+dr]$$

with $Q = w_d + \gamma(\phi - w_d)$. The random variable $N_{tot}(D)$ is the total number of users present in the same cell as the user at

the origin, when his distance from its serving base station is D. As users are distributed according to a PPP with intensity λ_u, $N_{tot}(D)$ is Poisson, with an intensity given by the conditional Palm expectation inside the integral.

Using Campbell's formula [22], this expectation becomes

$$E^0\Big[\int_0^\infty \int_0^{2\pi} \mathbf{1}_{(S(x,\theta)=S|r\leq D\leq r+dr)}\lambda_u d\theta x dx Q\Big] =$$

$$= \int_0^\infty \int_0^{2\pi} \lambda_u P(S(x,\theta)=S|r\leq D\leq r+dr) d\theta x dx Q$$

The conditional probability within the integral is given by the probability of being associate to one of the planar or vehicular base station, by taking into account our position in the origin. $\int_0^\infty \int_0^{2\pi} e^{-\lambda_b A(r,x,\theta)-2\pi\lambda_l \int_0^\rho 1-e^{-\mu_b\sqrt{\rho^2-t^2}}dt} d\theta x dx$, where $A(r,x,\theta)$ is given by:

$$A(r,x,\theta) =$$

$$\pi x^2 - \Big[r^2 \arccos\left(\frac{r+x\sin(\theta)}{d(r,x,\theta)}\right) + x^2 \arccos\left(\frac{x+r\sin(\theta)}{d(r,x,\theta)}\right) +$$

$$-\frac{1}{2}(-(d(r,x,\theta)-x)^2+r^2)^{\frac{1}{2}}((d(r,x,\theta)+x)^2-r^2)^{\frac{1}{2}}\Big]$$

while, since the formulation of PLCP is related to a well structured area with radius ρ it is possible to obtain that radius by starting from the created area A and by converting it into a circle with radius $\rho = \sqrt{\frac{A(r,x,\theta)}{\pi}}$. By substituting, we get the expression for $\bar{\tau}_d$.

The derivation of $\bar{\tau}_u$ follows along the same lines.The expressions of $\bar{\tau}_d$ and $\bar{\tau}_u$ obtained are implicit (i.e. they are a function of these same parameters). Thus they constitute a fixed point problem. It is easy to see however that the mapping operator associated to this fixed point is contractive, and thus that the problem admits a unique solution.

B. Proof of Theorem 2

Lemma 1. The average power received from users for the typical user arriving in the system at a distance r from the serving BS is approximated by

$$\bar{O} = \frac{(1-\gamma)\delta_u P_{bb} + \phi\gamma P_I}{(1-\gamma)\delta_u + \phi\gamma} \frac{(\lambda_b + \lambda_l\mu_b)\pi\alpha}{\alpha-2} \frac{\bar{\tau}_u}{\tau_u^0} \quad (21)$$

Proof. The mean transmit power from a user is $\frac{(1-\gamma)\delta_u P_{bb}+\gamma\phi P_I}{(1-\gamma)\delta_u+\gamma\phi}$. Let $x_i'(t), i \in \chi(j)$ be the position of the i-th user served by BS j at time t, $d(x,x_i'(t))$ denote the distance between the two users considered, and $u(x_i'(t))$ the probability that the given user is transmitting at time t. Then we can write the expression of $O(x,t)$ as

$$\sum_j \sum_{i\in\chi(j)} \frac{(1-\gamma)\delta_u P_{bb} + \gamma\phi P_I}{(1-\gamma)\delta_u + \gamma\phi} d(x,x_i'(t))^{-\alpha} u(x_i'(t)) \quad (22)$$

where $\chi(j)$ is the set of users served by BS j. As we assume the base station has utilization $\frac{\bar{\tau}_u}{\tau_u^0}$ in the uplink,

$$u(x_i'(t)) = \frac{1}{\lambda_u A_j}\frac{\bar{\tau}_u}{\tau_u^0}$$

where A_j is the area of the Voronoi cell of BS j. Given that users are uniformly distributed in the plane, the palm expectation of (22) is well approximated by

$$\frac{(1-\gamma)\delta_u P_{bb} + \gamma\phi P_I}{(1-\gamma)\delta_u + \gamma\phi} E\left[\sum_j \frac{\int_{x'\in A_j} d(x,x')^{-\alpha}dx'}{\lambda_u A_j}\right] \frac{\bar{\tau}_u}{\tau_u^0} =$$

As A_j is statistically independent on $d(x,x')$, the approximated formula becomes

$$= \frac{(1-\gamma)\delta_u P_{bb} + \gamma\phi P_I}{(1-\gamma)\delta_u + \gamma\phi} \frac{\int_0^{+\infty} \lambda_u min(1, s^{-\alpha}) 2\pi s ds}{\lambda_u \bar{A}} \frac{\bar{\tau}_u}{\tau_u^0}$$

where $\bar{A}$ is the mean area of a Voronoi cell for a BS density of λ_b, which is equal to λ_b^{-1}. Assuming $\alpha > 2$, we get

$$= \frac{(1-\gamma)\delta_u P_{bb} + \gamma\phi P_I}{(1-\gamma)\delta_u + \gamma\phi} \frac{(\lambda_b + \lambda_l\mu_b)\pi\alpha}{\alpha-2} \frac{\bar{\tau}_u}{\tau_u^0}$$

□

Proof. (Theorem 2) Let us rewrite expressions (5) to (7) in the form $h(x) = F(x) + K(x)Z(x)$. We have:

$$F_{TS}(x) = PD(x)^{-\alpha} L U_d(x) + I(x) + O(x)$$

$$Z_{TS}(x) = PD(x)^{-\alpha} U_d(x)(G\eta - L_g) +$$

$$-U_d(x)(1-\eta)(I(x)+O(x))$$

Let us consider first the TS case. Let's set

$$E^0[F(D)|r\leq D\leq r+dr] =$$

In the TS case, we have

$$PE^0[D(x)^{-\alpha} L U_d(x)|r\leq D\leq r+dr] =$$

$\forall x$, we approximate $U_d(x) = \frac{\bar{\tau}_d}{\tau_d^0}$. Thus

$$= Pr^{-\alpha} L_g \frac{\bar{\tau}_d}{\tau_d^0}$$

As for the remaining terms, we have

$$E^0[I(x)+O(x)|r\leq D\leq r+dr] =$$

$O(x)$ does not depend on the user distance from its serving BS. The expression of its expected value is thus given by Lemma 1. As for the conditional expectation of $I(x)$, it is given by (14) in Theorem 1, multiplied by reuse factor k. We thus have:

$$= k\bar{I}(r,k) + \bar{O}$$

For a given cell, $N_{tot}(D)$ is Poisson distributed. Thus the ratio of the standard deviation of over the mean of this variable decreases with increasing user density. Therefore in the dense IoT regime, such an inequality is tight. therefore, the denominator is then computed as a function of r as in the proof of Theorem 1. The derivation of the expressions for the DPS and SPS case follows along the same line. □